Formulation of Worst Spindle Speeds Considering Stability in End Milling

C. M. Zheng and J.-J. Junz Wang[*]

Department of Mechanical Engineering
National Cheng Kung University,
Tainan, Taiwan 701

jjwang@mail.ncku.edu.tw

Abstract - The frequency response function (FRF) is a representative characteristic of a self-excited vibration system, which has been well used to determine the worst spindle speeds and its corresponding critical limiting chip width for turning operation by finding the maximum negative real of FRF. In this study, the similar concept is extended to the 2 DOF milling system with planar isotropic dynamics on the X-Y plane, in which worst spindle speeds and its corresponding critical limiting axial depth of cut can be explicitly expressed in terms of cutting parameters and modal parameters. New frequency response function is developed by shifting a phase angle from the direct frequency response function multiplied by a magnitude factor in order to find critical limiting axial depth of cut and worst spindle speeds. Characteristic equation is derived to determine the value of the magnitude factor and phase angle, which is dependent of radial specific cutting constant and radial immersion angle. Also, this study provides a practical method for the estimation of process damping in milling operation.

Keywords - Milling, Chatter, Stability, Process damping, Radial factor matrix.

I. INTRODUCTION

Chatter or self-excited vibration in milling causes tool damage and poor surface finish and shortens machine tool life, which has plagued operators in shop. As shown in Fig. 1, vibration of the cutter causes a variable chip thickness which will give a variable cutting force and, subsequently, the variable cutting force leads a feedback to vibration of the cutter. Furthermore, the relative phasing between the surface waviness from one tooth to the next determines the level of vibration variation and whether the cutting process is stable or not. In other words, the reality of chatter can be regarded as the regeneration of surface waviness in cutting process. The first stability lobe diagram was proposed by Tobias and Fishwick [1], in which the spindle speed Ω versus limiting chip width $b_{\lim}$ family of curves separates the space into two regions. Any (Ω , $b_{\lim}$) pair that locates above the boundary is presumed to be unstable; while any pair below the boundary indicates stable machining. If we have the stability lobe diagram and choose the cutting conditions accordingly, then it is possible to avoid chatter. In order to develop stability lobe diagram for milling operation,

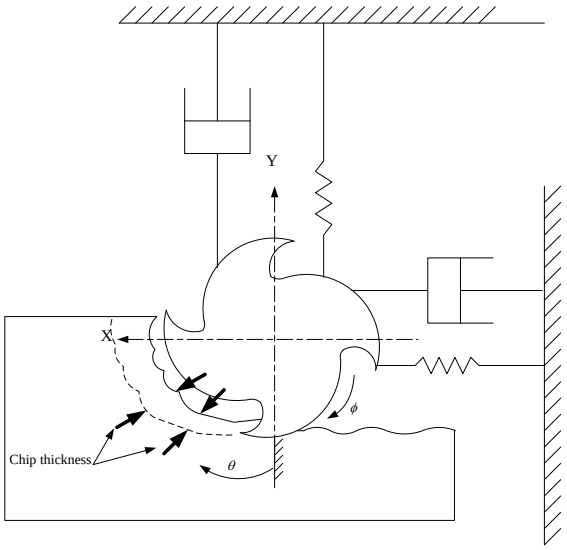

Fig.1 Chip thickness variation in milling

numerical simulation of chatter vibration is well recognized as an important technology, in which the cutter is divided into thin sections along axial axis and the instantaneous cutting force acting on each section is computed. Many numerical simulation methods in time domain have been developed to establish stability lobe diagram [2-5], in which cutting force can be considered to change with the vibration of cutter, regeneration of chip thickness and cutter runout effect. Although the numerical simulation provides the methods of the precise evaluation of the chatter vibration, it needs a time consuming computation. Furthermore, the onset of chatter may be identified hardly by observing changes in cutting forces or vibration displacements during several revolutions of cutting tool. In practice, it is difficult to analytically solve the stability problem for milling process, because the contact relations between workpice and cutting tool are changing as the cutting tool rotates. Comparing with turning process, a key barrier to provide an analytical solution for milling stability is the time dependence of the cutting force direction. Tlusty *et al.* [6-8] first solved this obstacle using average tooth angle approach. Assuming an average force direction and average number of teeth in the cut, stability analysis for turning process is modified to accommodate the milling process. Due to the assumption of the 'average' representations, time invariant system can be created to obtain stability lobe diagram algebraically for milling process. Minis and Yanushevsky [9] suggest an alternative analytical approach to calculate the time invariant system of milling operation. Applying Floquet theory and the generalized Nyquist stability criterion to the vibratory

[*] *Corresponding Author*
Email: jjwang@mail.ncku.edu.tw
Fax: 886-6-2367231

system, no assumptions with regard to the cutting force direction or number of teeth in cut are necessary. However, the work of Minis and Yanushevsky is called iterative analytical approach since the limiting chip width for selecting spindle speed is obtained through a few iterations. To arrive at "real" analytical approach for the prediction of chatter, Altintas and Budak [10-11] presented a direct prediction method in the frequency domain using the zero-order Fourier term to approximate the cutting force variation. The analytical approach is called zero-order solution (ZOS) and widely used by industry. Time-domain numerical simulation has confirmed that ZOS can achieve better accuracy than average tooth angle approach especially in the case of large radial immersion [12]. However, the algorithm described in ZOS for the calculation of stability lobes do not address explicit expressions for determining worst spindle speeds and its corresponding critical limiting chip width. Furthermore, in practical milling operations, process damping plays an important role in order to predict stability limit accurately. However, only a few papers focused on effect of process damping on the stability limit, and it has not been addressed that how to estimate the process damping. The objective of this study is to develop a closed form solution to determine worst spindle speeds and its corresponding critical limiting axial depth of cut. Based on the formulations of critical limiting axial depth of cut and worst spindle speeds, the method of estimating process damping is obtained. Also, the solution presented here can easily lend itself to the practical application to select better spindle speeds in milling.

A. Stability Analysis Based on Convolution Force Model

Based on the convolution integration concept, an analytical total force model for end milling process was established by Wang *et al.* [13]. Considering the cutter and workpiece to be rigid, Wang *et al.* express the milling force in a Fourier series expansion form:

$$\mathbf{f}(\phi)=\begin{pmatrix} f_x(\phi) \\ f_y(\phi) \end{pmatrix}=\sum_{k=-\infty}^{\infty}\begin{pmatrix} A_x(Nk) \\ A_y(Nk) \end{pmatrix}e^{jNk\phi} \tag{1}$$

Removing the assumption of a rigid cutter and expanding on the convolution model of Wang *et al.*, the total dynamic milling force for a rotating cutter can be expressed in a similar Fourier series expansion form

$$\mathbf{f}_d(\phi)=\begin{pmatrix} f_{dx}(\phi) \\ f_{dy}(\phi) \end{pmatrix}=\sum_{k=-\infty}^{\infty}\mathbf{A}_d[Nk]e^{jNk\phi}\begin{pmatrix} x_d(\phi-2\pi/N)-x_d(\phi) \\ y_d(\phi-2\pi/N)-y_d(\phi) \end{pmatrix} \tag{2}$$

where

$$\mathbf{A}_d[Nk]=\begin{bmatrix} A_{xx}(Nk) & A_{xy}(Nk) \\ A_{yx}(Nk) & A_{yy}(Nk) \end{bmatrix} \tag{3}$$

is the 2×2 complex Fourier coefficient matrix with the element $A_{ij}(Nk)$ representing the magnitude and phase of the kth harmonic component of the specific force in the i direction due to dynamic feed in the j direction and $T=2\pi/(N\Omega)$ is the tooth period of the cutter with a constant spindle speed, Ω .The average component of $\mathbf{A}_d$ matrix with k=0 in general have the highest magnitude and is of special significance in the stability analysis; they can be expressed in a simple closed form as follows:

$$\mathbf{A}_d[0]=\begin{bmatrix} A_{xx}(0) & A_{xy}(0) \\ A_{yx}(0) & A_{yy}(0) \end{bmatrix}=\frac{Nd_ak_t}{2\pi}\mathbf{P}[0] \tag{4}$$

where radial factor matrix $\mathbf{P}[0]$ can be shown to be

$$\begin{aligned}\mathbf{P}[0]&=\begin{bmatrix} 1 & k_r \\ -k_r & 1 \end{bmatrix}\begin{bmatrix} P_{11}(0) & P_{12}(0) \\ P_{21}(0) & P_{22}(0) \end{bmatrix} \\ &=\begin{bmatrix} 1 & k_r \\ -k_r & 1 \end{bmatrix}\begin{bmatrix} -0.25\cos 2\theta & -0.5\theta-0.25\sin 2\theta \\ 0.5\theta-0.25\sin 2\theta & 0.25\cos 2\theta \end{bmatrix}_{\theta=\theta_1}^{\theta_2}\end{aligned} \tag{5}$$

Using the average forces model with the assumption of planar symmetric structure on X-Y plane, the dynamic equation in second order form can be obtained as:

$$\begin{aligned}&\begin{bmatrix} m & 0 \\ 0 & m \end{bmatrix}\begin{pmatrix} x_d''(t) \\ y_d''(t) \end{pmatrix}+\begin{bmatrix} c & 0 \\ 0 & c \end{bmatrix}\begin{pmatrix} x_d'(t) \\ y_d'(t) \end{pmatrix}+\begin{bmatrix} k & 0 \\ 0 & k \end{bmatrix}\begin{pmatrix} x_d(t) \\ y_d(t) \end{pmatrix} \\ &=\frac{Nk_td_a}{2\pi}\begin{bmatrix} 1 & k_r \\ -k_r & 1 \end{bmatrix}\begin{bmatrix} P_{11}(0) & P_{12}(0) \\ P_{21}(0) & P_{22}(0) \end{bmatrix}\begin{pmatrix} x_d(t-T)-x_d(t) \\ y_d(t-T)-y_d(t) \end{pmatrix}\end{aligned} \tag{6}$$

According to the dynamic equation expressed by (6), regenerative chatter model in the Laplace domain can be described as shown in Fig. 2. The product of e^{-sT} and frequency response function matrix (FRF), $\mathbf{H}(s)=(1/ms^2+cs+k)\times\mathbf{I}_{2\times 2}$, serves as a feedback element of the regenerative chatter model and the feed forward loop of the model consists of a system gain, $Nk_td_a/2\pi$, and a plant, $\mathbf{P}[0]$.

Figure 2 depicts the representation of chatter as a closed loop system and states characteristic equation for onset of chatter in explicit expression of the cutting parameters and the structure parameters as follow:

$$\det\left(\mathbf{I}_{2\times 2}+\frac{Nk_td_a}{2\pi}(1-e^{-sT})\begin{bmatrix} \lambda_1 & 0 \\ 0 & \lambda_2 \end{bmatrix}\mathbf{H}(s)\right)=0 \tag{7}$$

where λ_1 and λ_2 are the eigenvalues of matrix $\mathbf{P}[0]$. Computing the determinant, an expression is given as

$$[1+\frac{Nk_td_a}{2\pi}(1-e^{-sT})\lambda_1H(s)][1+\frac{Nk_td_a}{2\pi}(1-e^{-sT})\lambda_2H(s)]=0 \tag{8}$$

where $H(s)=(1/ms^2+cs+k)$. From (8), It has been shown that the characteristic equation in Eq. (7) for 2 DOF milling system can be resolved into two quasi-one-dimensional characteristic equations:

$$\begin{aligned}&1+\frac{Nk_td_a}{2\pi}(1-e^{-sT})\lambda_1H(s)=0 \\ &\qquad\qquad or \\ &1+\frac{Nk_td_a}{2\pi}(1-e^{-sT})\lambda_2H(s)=0\end{aligned} \tag{9}$$

From these two available characteristic equations, the smaller d_a value for the onset of chatter is selected to define the stability boundary. Thus, the corresponding eigenvalue to the smaller d_a value is used to obtain the analytical expressions for the critical limiting axial depth of cut in next section.

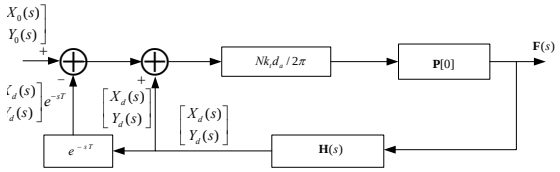

Fig. 2. Block diagram of milling system with regenerative chatter

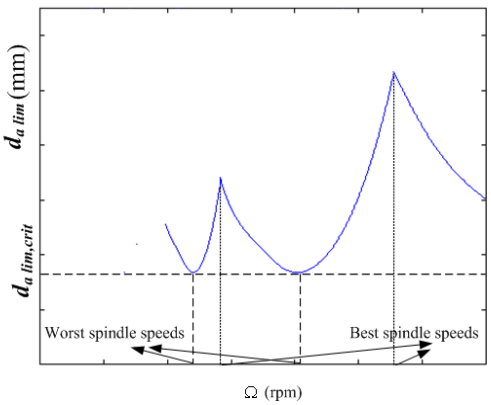

Fig. 3. Typical stability lobe diagram

II. FORMULATION OF CRITICAL LIMITING AXIAL DEPTH OF CUT

Figure 3 depicts a typical stability lobe diagram, in which the minimum $d_{a\,lim}$ value is called critical limiting axial depth of cut, $d_{a\,lim,crit}$., and the spindle speeds where the $d_{a\,lim,crit}$ encountered are referred to worst spindle speeds. On the other hand, the spindle speeds corresponding to peaks of stability lobes are called best spindle speeds.

According to the expression of (5), the eigenvalues of **P**[0] are a function of specific cutting force ratio, k_r, entry cutting angle, θ_1, and exit cutting angle, θ_2, which can be determined using quadratic equation as follow:

$$\lambda^2 - k_r\theta_r\lambda + (1+k_r^2)(\theta_r^2/4 - s_r^2 - c_r^2) = 0 \tag{10}$$

where

$$\begin{aligned} \theta_r &= \theta_2 - \theta_1 \\ s_r &= [\sin(2\theta_2) - \sin(2\theta_1)]/4 \\ c_r &= [\cos(2\theta_2) - \cos(2\theta_1)]/4 \end{aligned} \tag{11}$$

Equation (10) is solved for λ to obtain the eigenvalues:

$$\lambda_1,\ \lambda_2 = \frac{k_r\theta_r \pm \sqrt{(1+k_r^2)\sin^2\theta_r - \theta_r^2}}{2} \tag{12}$$

Note that the eigenvalues presented in (12) are not limited to real number; it is generic to complex number. Therefore, the eigenvalues can be expressed in the generalized form with a complex conjugate pair:

$$\lambda_1,\ \lambda_2 = \frac{k_r\theta_r \pm j\psi}{2} \tag{13}$$

where

$$\psi = \sqrt{\theta_r^2 - (1+k_r^2)\sin^2\theta_r} \tag{14}$$

For illustration purpose, assuming λ_1 is applied to determine the stability boundary, and thus Eq. (14) can be rewritten as

$$\begin{aligned} \lambda_1 H(s) &= |\lambda_1| e^{j\theta_\lambda} H(s) = e^{j\theta_\lambda} H_1(s) = \tilde{H}(s) \\ &= \frac{-2\pi}{Nk_t d_a (1 - e^{-sT})} \end{aligned} \tag{15}$$

where

$$|\lambda_1| = \frac{\sqrt{(k_r\theta_r)^2 + \psi^2}}{2}, \qquad \theta_\lambda = \tan^{-1}\left(\frac{\psi}{k_r\theta_r}\right) \tag{16}$$

Equation (15) shows that the modified frequency response function $\tilde{H}(s)$ is the transforming result of $H(s)$ from two step transformation. The first transformation $H_1(s) = |\lambda_1| H(s)$ scales $H(s)$ by the positive constant $|\lambda_1|$, it experiences a uniform magnification if $|\lambda_1|$>1 and a uniform contraction if $|\lambda_1|$ <1. When $e^{j\theta_\lambda}$ is multiplied $H_1(s)$ is added, the second transformation $\tilde{H}(s) = e^{j\theta_\lambda} H_1(s)$ produces a uniform rotation through an angle θ_λ about the origin of H (s) on the complex plane. Applying Nyquist criterion to the onset of chatter, which implies that $s = j\omega_c$, then the $\tilde{H}(s)$ is given by

$$\tilde{H}(s) = \tilde{H}(\omega_r) = \tilde{U}(\omega_r) + j\tilde{V}(\omega_r) \tag{17}$$

where $\omega_r = \omega_c / \omega_n$ is the ratio of chatter frequency ω_c to nature chatter frequency ω_n. The real and imaginary parts of $\tilde{H}(\omega_r)$ can be expressed as

$$\begin{aligned} \tilde{U}(\omega_r) &= |\lambda_1|[U(\omega_r)\cos\theta_\lambda - V(\omega_r)\sin\theta_\lambda] \\ \tilde{V}(\omega_r) &= |\lambda_1|[U(\omega_r)\sin\theta_\lambda + V(\omega_r)\cos\theta_\lambda] \end{aligned} \tag{18}$$

where

$$\begin{aligned} U(\omega_r) &= \frac{1}{k}\frac{1-\omega_r^2}{(1-\omega_r^2)^2 + (2\zeta\omega_r)^2} \\ V(\omega_r) &= \frac{1}{k}\frac{-2\zeta\omega_r}{(1-\omega_r^2)^2 + (2\zeta\omega_r)^2} \end{aligned} \tag{19}$$

where k and ζ are denoted as stiffness and damping ratio respectively. The $U(\omega_r)$ and $V(\omega_r)$ represent the real and imaginary parts of $H(\omega_r)$ which is obtained by substituting $s = j\omega_c$ into $H(s)$. In (15), replacing $\tilde{H}(s)$ by $\tilde{H}(\omega_r)$ via $s = j\omega_c$ and equating real and imaginary parts of the equation gives

$$\frac{-\pi}{Nk_t d_a} = \tilde{U}(\omega_r) \tag{20}$$

$$\frac{\pi}{Nk_t d_a}\frac{\sin\omega_c T}{1-\cos\omega_c T} = \tilde{V}(\omega_r) \tag{21}$$

Given (20), the smallest value d_a on stability boundary of stability lobes diagram can be determined by finding the maximum negative real of $\tilde{U}(\omega_r)$. Therefore, setting $\frac{d\tilde{U}(\omega_r)}{d\omega_r} = 0$ shows that

$$\frac{-2\omega_{rc}[(1-\omega_{rc}^2)^2 + (2\zeta\omega_{rc})^2] + 4\omega_{rc}(1-\omega_{rc}^2)[(1-\omega_{rc}^2) - 2\zeta^2]}{-2\zeta[(1-\omega_{rc}^2)^2 + (2\zeta\omega_{rc})^2] - 8\zeta\omega_{rc}^2(1-\omega_{rc}^2)[(1-\omega_{rc}^2) - 2\zeta^2]} = \tan\theta_\lambda \tag{22}$$

where ω_{rc} is the chatter frequency ratio corresponding to critical limiting axial depth of cut. Although the Eq. (22) relates ω_{rc}, ζ and θ_λ as an algebraic equation, it is more helpful for this study to express ω_{rc} directly as a function of ζ and θ_λ by the form as:

$$\omega_{rc} = \Psi(\zeta, \theta_\lambda) \tag{23}$$

It seems to be a difficult task to obtain an exact solution for the $\Psi(\zeta, \theta_\lambda)$. Therefore, looking for an approximate solution for the $\Psi(\zeta, \theta_\lambda)$ may be a viable way. In order to find an appropriate simplification, it is necessary to clarify the range of θ_λ in (22) before starting the derivation of the approximate solution for the $\Psi(\zeta, \theta_\lambda)$. The λ value in (13)

is presented in two possible cases, a real number or complex number. The range of θ_λ can then be determined for this two cases. If λ is a real number, then $\lambda_1 = (k_r\theta_r + \sqrt{(1+k_r^2)\sin^2\theta_r - \theta_r^2})/2$ must be a positive real number to make physical sense. However, further examination is needed to determine whether $\lambda_2 = (k_r\theta_r - \sqrt{(1+k_r^2)\sin^2\theta_r - \theta_r^2})/2$ is a positive real number or not. If λ_2 is a positive real number, following relationship must be satisfied:

$$k_r\theta_r > \sqrt{(1+k_r^2)\sin^2\theta_r - \theta_r^2} \tag{24}$$

After rearranging (24), a simple relationship can then be written as

$$\theta_r > \sin\theta_r \tag{25}$$

Equation (25) shows that whether λ_2 is a positive real number or not depends only on radial immersion angle, with nothing more than the radial specific cutting constant, k_r. Let $\theta_{rr} = \theta_r - \sin\theta_r$, θ_{rr} is always greater than zero for all radial immersions, $0^0 < \theta_r \le 180^0$. This shows that λ_2 must be a positive real number. The above discussions show that λ must be a positive real number if λ is a real number. In other words, θ_λ is equal to zero when λ is a real number. For the second case, assuming that λ is a complex number, the real part of λ, $k_r\theta_r$, must be a positive real number to make physical sense. Therefore, the possible region of θ_λ is in $-90^0 \le \theta_\lambda \le 90^0$ when λ is a complex number. Recall that θ_λ is equal to zero when λ is a real number, which is included in the region, $-90^0 \le \theta_\lambda \le 90^0$. Based on the above discussions, the phase angle θ_λ must be limited to the region, $-90^0 \le \theta_\lambda \le 90^0$, when mapping $H(s)$ to $\tilde{H}(s)$. In addition, the damping ratio in milling is less than 0.1 in practice. Based on the assumption of the small damping ratios, substituting damping ratios 0.02, 0.04, 0.06 and 0.08 into (22), an almost linear relationship between ω_{rc} and θ_λ in the region $-90^0 \le \theta_\lambda \le 90^0$ is obtained as shown in Fig. 4.Therefore, it shows that even though Eq. (22) describes non-linear relationship between ω_{rc} and θ_λ but behaves qualitatively like linear relationship in the region $-90^0 \le \theta_\lambda \le 90^0$ when the damping ratio is less than 0.1. The approximation of Eq. (22) for the linear relationship can be written as

$$\omega_{rc} = a_0\theta_\lambda + b_0 \tag{26}$$

According to the nature of linear function, if two points, $(\omega_{rc1}, \theta_{\lambda 1})$ and $(\omega_{rc2}, \theta_{\lambda 2})$, on the line is given, then a_0 and b_0 can be determined. Substituting $\theta_{\lambda 1} = 0$ into (22), this simplifies to $\omega_{rc1} = \sqrt{1+2\zeta}$. Similarly, substituting $\omega_{rc2} = 1$ into (22), this simplifies to $\theta_{\lambda 2} = \tan^{-1}(\frac{-1}{\zeta})$. Once the two points, $(\omega_{rc1}, \theta_{\lambda 1})$ and $(\omega_{rc2}, \theta_{\lambda 2})$, are given, the

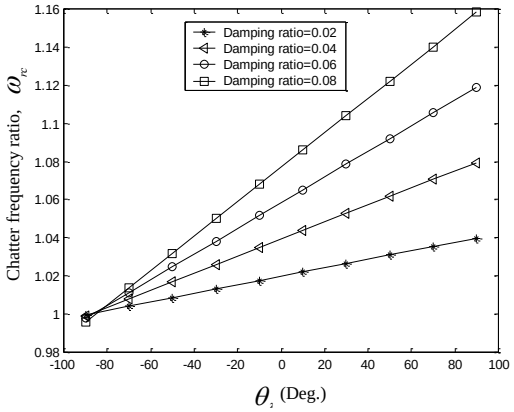

Fig. 4. Variation of ω_{rc} with θ_λ at various damping ratios

values of a_0 and b_0 can be solved, and (26) thus can be rewritten as

$$\omega_{rc} = \sqrt{1+2\zeta} - \frac{\sqrt{1+2\zeta}-1}{\tan^{-1}(\frac{-1}{\zeta})}\theta_\lambda \tag{27}$$

Due to the assumption of a small damping ratio ($\zeta < 0.1$), $\sqrt{1+2\zeta}$ and $\tan^{-1}(-1/\zeta)$ can be approximated as $1+\zeta$ and $-\pi/2$ respectively, and then (27) can be further simplified as

$$\omega_{rc} = 1 + \zeta(1 + \frac{2\theta_\lambda}{\pi}) \tag{28}$$

Substituting (28) into (20), critical limiting axial depth of cut, $d_{a\ lim,crit}$, can be shown to be:

$$da_{\text{lim, }crit} = \frac{2\pi}{Nk_t|\lambda_1|}\frac{k\zeta[1+(1+\frac{2\theta_\lambda}{\pi})^2]}{(1+\frac{2\theta_\lambda}{\pi})\cos\theta_\lambda - \sin\theta_\lambda} \tag{29}$$

Equation (29) shows that the critical limiting axial depth of cut is proportional to stiffness k and damping ratio ζ, and is inversely proportional to flute number of cutter N and tangential specific cutting constant k_t. This equation also describes that stiffness and damping ratio is of equal importance to the critical limiting axial depth of cut in milling. In other words, (29) states that the best stability can be obtained when the product of stiffness and damping ratio has a maximum value. This point is particular worthy of attention for the design of fixture-clamping or tool-holding, because the general designer may only focus on the stiffness while ignoring the importance of damping ratio. Due to the existence of process damping, actual damping ratio in milling may be not equal to the damping ratio identified from impact test. Actual damping ratio can be easily estimated by applying (29) once critical limiting axial depth of cut, $d_{a\ lim,crit}$, is given from cutting test. Before finding critical limiting axial depth of cut through cutting test, the worst spindle speeds corresponding to critical limiting axial depth of cut must be determined. The derivation of worst spindle speeds is presented in next section.

III. IDENTIFICATION OF WORST SPINDLE SPEEDS

Using ω_{rc} instead of ω_r in (21) and substituting (29) into (21) yields the following equation:

$$\frac{\sin(\omega_{rc}T_c)}{1-\cos(\omega_{rc}T_c)} = \frac{c_0\sin\theta_\lambda + \cos\theta_\lambda}{\sin\theta_\lambda - c_0\cos\theta_\lambda} \tag{30}$$

where $c_0 = 1+2\theta_\lambda/\pi$ is between 0 and 2, which is dependent of radial immersion angle. The $T_c = 2\pi/N\Omega_{worst}$ represents time period corresponding to critical limiting axial depth of cut. Using trigonometric identities, (30) can be rewritten as

$$\cos(\omega_{rc}T_c) = \frac{2c_0\sin 2\theta_\lambda + (1-c_0^2)\cos 2\theta_\lambda}{1+c_0^2} \tag{31}$$

Substituting (28) and $T_c = 2\pi/N\Omega_{worst}$ into Eq. (31), the worst spindle speed, Ω_{worst}, is written as:

$$\Omega_{worst} = \frac{2\pi\omega_n(1+c_0\zeta)\times 60}{N[\frac{3\pi}{2}+2\theta_\lambda+\tan^{-1}(\frac{1-c_0^2}{2c_0})]} \tag{32}$$

where Ω_{worst} is given in rpm and ω_n in Hz . Note that the Ω_{worst} in (32) is one of the worst spindle speeds considering the cutting condition with $0 \le \omega_{rc}T_c \le 2\pi$. In general case, the worst spindle speeds at *n*th stability lobe can be expressed as:

$$\Omega_{worst,n} = \frac{2\pi\omega_n(1+c_0\zeta)\times 60}{N\{[\frac{3\pi}{2}+2\theta_\lambda+\tan^{-1}(\frac{1-c_0^2}{2c_0})]+2(n-1)\pi\}} \tag{33}$$

Comparing (29) with (33), it can be found that damping ratio has very different effects on critical limiting axial depth of cut and worst spindle speeds. For example, as ζ increases from 0.02 to 0.04, critical limiting axial depth of cut increases by 1 times while worst spindle speeds increase slightly by 4% (considering the extreme case, $c_0 = 2$). In other words, critical limiting axial depth of cut is very sensitive to the changes in damping ratio, but damping ratio has little effect on worst spindle speeds. Thus, (33) can be simplified as:

$$\Omega_{worst,n} = \frac{2\pi\omega_n\times 60}{N\{[\frac{3\pi}{2}+2\theta_\lambda+\tan^{-1}(\frac{1-c_0^2}{2c_0})]+2n\pi\}} \tag{34}$$

Once worst spindle speeds and the corresponding critical limiting axial depth of cut are given, identification of process damping can be performed at a worst spindle speed from the measured critical limiting axial depth of cut.

The detail of cutting tests for identification of process damping is presented in next section.

IV. EXPERIMENTAL VALIDATION

Milling experiments were carried out with 3-axis vertical milling machine. A two-fluted tungsten carbide end-mill of 20 mm diameter and 15 degrees helix angle was used in milling the SKD61. Measured signals from the accelerometer are used to determine whether the milling is stable or unstable. Beginning of the experiment is to identify specific cutting constants, which is an important task for predicting stability lobe diagram. The method for the estimation of shearing and ploughing cutting constants presented by Wang and Zheng [14] is used in this study. The tangential and radial specific cutting coefficients are identified as 1570 N/mm^2 and 0.343 respectively. The real and imaginary parts of the FRFs were measured to identify the modal parameters using peak-picking method. Identification results shows that the rigidity of workpice is 100 times more than the cutting tool, so it is reasonable to assume the workpice as a rigid body. There are three apparent modes of the cutting tool measured at the end of the mill at 592 Hz, 1130 Hz and 1200 Hz and almost equally appear in the X and Y directions. The 1200 Hz mode is the most prominent mode, thus the modal parameters of the 1200 Hz mode listed in Table 1 are used to predict stability diagram. Cutting tests were carried out in down milling with 50% radial immersion, and thus λ_1, $\lambda_2 = 0.269 \pm 0.58j$ can be found from (13). Substituting λ_1 and λ_2 into (29), the corresponding critical limiting axial depth of cut are found to be 1.82 mm and -38 mm respectively. Note that the value -38mm does not make physical sense, and then the predicted critical limiting axial depth $d_{a\,lim,crit}$ is 1.82mm. Furthermore, substituting $\lambda_1 = 0.269 - 0.58j$ into (33), the worst spindle speeds can be obtained and listed in Table 2 as spindle speed ranges from 1900 rpm to 2500 rpm. In order to verify the formulae presented in (29) and (33), stability lobe diagram from ZOS method [10] is developed as shown in Fig. 5. Comparing Table 2 and Fig. 5, it can be found that the critical limiting axial depth and its corresponding worst spindle speeds predicted by this study agree very well with the results from ZOS method. In order to confirm the predicted critical limiting axial depth and worst spindle speeds, the spindle speeds 2150 rpm, 2175 rpm and 2230 rpm were firstly selected to conduct the milling tests. As shown in Fig. 5, although changes of limiting axial depth of cut in the trend agree with predicted results, the measured critical axial depth of cut from milling test at 2175 rpm is about twice the predicted value of 1.82 mm. Based on the (29), the inaccurate prediction for critical axial depth of cut may result from the effect of process damping. If it is true, the total damping is about twice the modal damping 0.0075, which implies that process damping is about equal to modal damping. To verify the above reasoning, the damping ratio is revised from 0.0075 to 0.015 and used to predict the stability lobe diagram by ZOS method. Comparing new stability lobe diagram with experiment results, the predicted values agree well with the experiment results as shown in Fig. 6 Comparing stability lobe diagrams in Fig. 5 and Fig. 6, as damping ratio increases from 0.0075 to 0.015, critical limiting axial depth of cut increases by 1 times while the worst spindle speeds vary slightly with damping ratio as presented in section C.

Table 1 Modal parameters of 1200 Hz mode identified from impact testing

Nature frequency, ω_n (Hz)	Stiffness, k (N/m)	Damping ratio, ζ
1200	7.4×10^7	0.0075

Table 2 Worst spindle speeds between 1900 rpm and 2500 rpm

n	18	17	16	15	14
Worst spindle speed (rpm)	1941	2051	2175	2315	2474

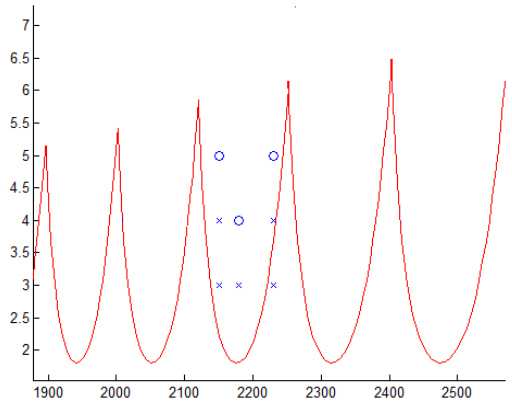

Fig.5 Comparison of experimental results and stability lobe diagram from ZOS [10] using damping ratio=0.0075, '×': Conducted experiment in stable milling , 'O': Conducted experiment in unstable milling

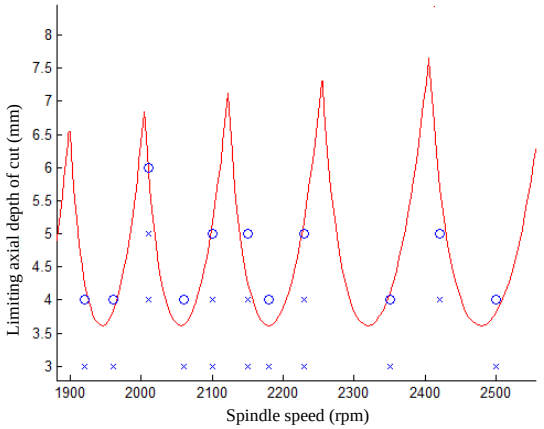

Fig.6 Comparison of experimental results and stability lobe diagram from ZOS [10] using damping ratio=0.015, '×': Conducted experiment in stable milling , 'O': Conducted experiment in unstable milling.

Apparently, there is a best spindle speed $\Omega_{best,n}$ corresponding to the nth lobe between $\Omega_{worst,n}$ and $\Omega_{worst,n+1}$, and $\Omega_{best,n}$ can be roughly written by

$$\Omega_{best,n} = \Omega_{worst,n} + 0.6(\Omega_{worst,n+1} - \Omega_{worst,n}) \quad (35)$$

Although the selected spindle speed by (35) does not match the best spindle speed exactly, the selection can be near the best spindle speed at least.

V. CONCLUSIONS

In this study, combining the convolution force model and the dynamics of 2 DOF milling system, two quasi-one-dimensional characteristic equations are derived to find the critical axial depth of cut and its corresponding spindle. Based on the formulation of critical limiting axial depth of cut, it shows that the best stability can be obtained when the product of stiffness and damping ratio has a maximum value. In practice, critical limiting axial depth of cut is very sensitive to the changes in damping ratio while damping ratio has little effect on worst spindle speeds. Also, Based on the formulations of critical limiting axial depth of cut and worst spindle speeds, this study provides a practical method to estimate process damping in milling.

Acknowledgment

The authors gratefully acknowledge the financial support from National Science Council of Taiwan through Grant No. NSC 99-2212-E-006-019.

REFERENCES

[1] Tobias, S. A. and Fishwick, W., "Theory of Regenerative Machine Tool Chatter," Engineering, 205 (1958) 199-203.

[2] Liao, Y. S. and Young, Y. C., "A New On-line Spindle Speed Regulation Strategy for Chatter Control," International Journal of Machine Tools & Manufacture, 36/5 (1996) 651-660.

[3] Davies, M. A., Pratt, J. R., Dutterer, B. And Burns, T. J., "Stability Prediction for Low Radial Immersion Milling," ASME Journal of Manufacturing Science and Engineering, 124 (2002) 217-225.

[4] Insperger, T., Stépán, G.; "Updated Semi-discretization Method for Periodic Delay-differential Equations with Discrete Delay," International Journal of Numerical Methods in Engineering, 61/1 (2004) 117-141.

[5] Ding, Y., Zhu, L., Zhang, X. and Ding, H., "Numerical Integration Method for Prediction of Milling Stability," ASME Journal of Manufacturing Science and Engineering, 133 (2011) 31005-31012.

[6] Tlusty, J., Zaton, W. and Ismail, F., "Stability Lobes in Milling," Annals of the CIRP, 32/1 (1983) 309-313.

[7] Smith, K. S. and Tlusty, J., "Update on High Speed Milling Dynamics," ASME Journal of Engineering for Industry, 112 (1990) 142-149,.

[8] Smith, K. S. and Tlusty, J., "An Overview of Modeling and Simulation of the Milling Process," ASME Journal of Engineering for Industry, 113 (1991) 169-175.

[9] Minis, I. and Yanushevsky, T., "A New Theoretical Approach for the Prediction of Machine Tool Chatter in Milling," ASME Journal of Engineering for Industry, 18 (1993) 1-8.

[10] Budak, E and Altintas, Y., "An Analytical Prediction of Chatter Stability in Milling – Part I: General Formulation," ASME Journal of Dynamic Systems, Measurement and Control, 120 (1998) 22-30.

[11] Budak, E. and Altintas, Y., "An Analytical Prediction of Chatter Stability in Milling – Part II: Application of the General Formulation to Common Milling Systems," ASME Journal of Dynamic Systems, Measurement and Control, 120 (1998) 31-36,.

[12] Schmitz, T. L. and Smith, K. S., Machining Dynamics, Springer Publishing Co., New York, (2008).

[13] Wang, J.-J., Liang, S.Y. and Book, W.J., "Convolution Analysis of Milling Force Pulsation," ASME Journal of Engineering for Industry, 116 (1994) 17-25.

[14] Wang, J. -J. Junz and Zheng, C.M., "An Analytical Force Model with Shearing and Ploughing Mechanisms for End Milling," International Journal of Machine Tools and Manufacture, 42 (2002) 761-771.